J Neuropathol Exp Neurol
Vol. 00, No. 00, May 2020, pp. 1–15
doi: 10.1093/jnen/nlaa050

ORIGINAL ARTICLE

Numbers of Axons in Spared Neural Tissue Bridges But Not Their Widths or Areas Correlate With Functional Recovery in Spinal Cord-Injured Rats

Svenja Rink, MD, Stoyan Pavlov, MD, PhD, Aliona Wöhler, MD, Habib Bendella, MD, Marilena Manthou, MD, Theodora Papamitsou, MD, Sarah A. Dunlop, PhD, and Doychin N. Angelov, MD, PhD

Abstract

The relationships between various parameters of tissue damage and subsequent functional recovery after spinal cord injury (SCI) are not well understood. Patients may regain micturition control and walking despite large postinjury medullar cavities. The objective of this study was to establish possible correlations between morphological findings and degree of functional recovery after spinal cord compression at vertebra Th8 in rats. Recovery of motor (Basso, Beattie, Bresnahan, foot-stepping angle, rump-height index, and ladder climbing), sensory (withdrawal latency), and bladder functions was analyzed at 1, 3, 6, 9, and 12 weeks post-SCI. Following perfusion fixation, spinal cord tissue encompassing the injury site was cut in longitudinal frontal sections. Lesion lengths, lesion volumes, and areas of perilesional neural tissue bridges were determined after staining with cresyl violet. The numbers of axons in these bridges were quantified after staining for class III β-tubulin. We found that it was not the area of the spared tissue bridges, which is routinely determined by magnetic resonance imaging (MRI), but the numbers of axons in them that correlated with functional recovery after SCI (Spearman's $\rho > 0.8$; $p < 0.001$). We conclude that prognostic statements based only on MRI measurements should be considered with caution.

Key Words: Correlation analysis, Functional recovery, Neurotubulin content, Spared white matter, Spinal cord injury.

INTRODUCTION

Traumatic spinal cord injury (SCI) destroys tissue directly via the initial impact as well as via subsequent secondary degeneration that evolves over time and results in a range of motor and sensory deficits with various degrees of severity (1). Both gray and white matter are adversely affected, which, depending on the vertebral level, leads to deficits in multiple organ systems (2,3). Furthermore, recent MRI imaging in humans has shown that after cervical injury, degeneration also occurs remotely in the lumbar spinal cord, emphasizing the widespread nature of this injury (4). There are currently no definitive regenerative or restorative interventions that markedly improve outcome following SCI (5). Current options include primarily medical management and rehabilitation (2), as well as increasing emphasis on sensory stimulation (6).

Studies primarily in rodent models have shown that, although lesions of differing severity result in an initial complete loss of motor, sensory and vegetative function, partial recovery to varying degrees nevertheless often ensues (7–10). This provides the opportunity to examine whether any morphological factors underpin functional recovery.

A notable feature in any contusion model is that a small perilesional rim of spared tissue often remains, even following severe injury (11–17). Survival of such perilesional neural tissue bridges (PNTB) has also been recognized in human SCI pathology, where there is some tissue sparing even in neurologically complete patients that are categorized as "discomplete" (18–21). PNTBs are the target of acute treatments that attempt to delay or slow secondary degeneration, thus preserving intact fibers and therefore function (22). Simi-

1From the Department of Prosthetic Dentistry, School of Dental and Oral Medicine, University of Cologne, Germany (SR); Department of Anatomy, Histology and Embryology, Medical University, Varna, Bulgaria (SP); Department of Anatomy I, University of Cologne (AW, DNA); Department of Neurosurgery, University of Witten/Herdecke, Cologne Merheim Medical Center (CMMC), Cologne (HB), Germany; Department of Histology and Embryology, Aristotle University Thessaloniki, Greece (MM, TP); and School of Biological Sciences, The University of Western Australia, Australia (SAD).

Send correspondence to: Doychin N. Angelov, MD, PhD, Department of Anatomy I, University of Cologne, Institut 1 für Anatomie der Universität zu Köln, Joseph-Stelzmann-Strasse 20, D-50931 Köln, Germany; E-mail: angelov.anatomie@uni-koeln.de

Svenja Rink and Stoyan Pavlov contributed equally and share first authorship. Sarah A. Dunlop and Doychin N. Angelov contributed equally and share senior authorship.

Dr. med. Habib Bendella was financially supported by the Interne Forschungsförderung (IFF) der Universität Witten/Herdecke (IFF2017-08) and Dr. med. dent. Svenja Rink by grant Nr. 410/2017 of the Köln Fortune Program, University of Cologne.

The authors have no duality or conflicts of interest to declare.

Supplementary Data can be found at academic.oup.com/jnen.

larly, chronic treatments are targeted to either add to these spared fibers or use rehabilitation to enhance any residual function (6,23).

The objective of this study was therefore to analyze deficits in locomotion, sensitivity and vegetative functions after graded incomplete bilateral spinal cord lesions in adult rats and to relate these to morphological findings (i.e. lesion volume, lesion length, PNTB area, and number of axons in PNTB).

MATERIALS AND METHODS

Overview of Animal Groups

Thirty-two adult (175–200 g) female Wistar rats (strain HsdCpb: WU, Harlan, An Venray, The Netherlands) were used. All animals were subjected to a single spinal cord compression injury to 50% of its diameter at 3 different impact speeds: 50 mm/second (SCI-50: 8 rats), 75 mm/second (SCI-75: 12 rats), and 100 mm/second (SCI-100: 12 rats).

Data from our earlier experiments, provided the basis for our statistical analysis for which we used G*Power Version 3.1.4 (Franz Faul, University of Kiel, Kiel, Germany) (24). In the previous study, using a contusion velocity of 100 mm/second for 1 second, rump-height index (RHI) at 2 months after SCI was 2.82 ± 0.13 points. We predicted that, in the course of recovery, RHI would reach 4.50 points, corresponding to an effect strength of 3.36. We expected that the minimal relevant effect that we would be able to detect would be 0.5 points, which corresponds to an effect strength of 1.4. For this comparison, a *t*-test requires 7–9 rats per group. In this case, significant differences would be detected with a power of 80% with a type 1 error of 5%.

Animals were fed standard laboratory food (Ssniff Spezialdiäten, Soest, Germany), provided tap water ad libitum and kept at 23°C on a 12-hour artificial light-dark cycle. All experiments were conducted in accordance with German Law on the Protection of Animals. Procedures were approved by the local Animal Care Committee (approval number 84-02.04.2014.A348). Functional recovery was examined in all rats at 1, 3, 6, 9, and 12 weeks after SCI.

Prelesion Training (Conditioning)

As described in detail previously (24–27), prior to SCI surgery, all rats underwent daily conditioning for 2 weeks, including training to walk on a wooden beam, climb a ladder, and stay still in the transparent chamber of the Thermal Plantar Analgesia Instrument (Ugo Basile Thermal Plantar Analgesia Instrument, Stoelting Europe, Dublin, Ireland), for sensory measurements. All animals rapidly became accustomed to the tasks within 2–3 days and did not show any signs of stress, such as freezing, trying to bite, weight loss, or lack of grooming.

Spinal Cord Injury

We adopted a transient spinal cord compression method (28) and have used it routinely in our laboratory (24,27,29). Briefly, rats were anesthetized (1.8 vol% Isofluorane: Forene, Abbott Laboratories, Chicago, IL, 0.6 L/minute O_2: Conoxia and 1.2 L/minute N_2O: Niontix, Linde, Dublin, Ireland). A laminectomy was performed at the eighth thoracic vertebra and the exposed 10th thoracic spinal cord segment (i.e. at the level of the eighth thoracic vertebra [30]) compressed at a velocity of 50, 75, or 100 mm/second for 1 second using electromagnetically controlled watchmaker forceps (Dumont #5, Fine Science Tools, Heidelberg, Germany); closure was controlled to be 50% of spinal cord diameter.

We used this method to induce mild (SCI-50: velocity of 50 mm/second), moderate (SCI-75: 75 mm/second), or severe (SCI-100: 100 mm/second) bilateral spinal cord contusion injury. The use of 3 different severities allowed us to identify which model would cause abrupt initial disability followed by a gradual ongoing recovery thereby providing the opportunity to determine whether there were any associations between functional recovery and lesion site characteristics (i.e. length, volume, PNTB area, numbers of antineuronal class III β-tubulin-positive profiles).

This compressive bilateral injury affects both corticospinal tracts in the dorsal white matter funiculus (31) and the reticulospinal tract which projects within the ventrolateral funiculus, and determines the degree of locomotor deficit (32–35). To prevent hypothermia, rats were kept at 37°C for 12 hours and then housed individually in standard cages. Manual bladder voiding was undertaken twice daily at ∼7:00 and ∼19:00 until the end of the experiment, that is, 12 weeks after SC surgery.

Assessments

All functional and anatomical analyses were undertaken by 2 independent investigators blinded to treatment group.

Functional Assessments

Locomotor Performance

Locomotor function was measured prior to SCI (0 weeks) and at 1, 3, 6, 9, and 12 weeks thereafter using the Basso, Beattie, Bresnahan (BBB) rating scale (7) and beam-walking as described previously (24,27). Video recordings (Panasonic NV-DS12, Panasonic Corporation, Kadoma, Osaka, Japan, at 25 frames per second) of the animal's left and right side were made, observed at slow playback speed and scores for the left and right extremities were averaged (27).

Selected frames within a single frame motion analysis were used to measure foot stepping angle (FSA), which is an objective measure of stepping (plantar or dorsal) and a major attribute of the BBB score. The FSA is the angle at which animals place their hind paw on the ground at the beginning of the stance phase. The angle is defined by a line parallel to the paw's dorsal surface and the horizontal axis measured from video frames in which the paw is seen in initial firm contact with the ground. In intact rats, the stance phase is well defined and the angle <20°. After SCI, rats drag their hind limbs with dorsal paw surfaces facing the beam surface and the FSA is increased to 130°–140°. In severely disabled rats, "step cycles" were defined by the movements of the forelimbs. Video

frames in which the angle appeared to have its lowest values for individual "cycles," typically following a visible attempt to flex the extremity, were used for measurements. In the less severely disabled rats that performed stepping of variable quality (dorsal or plantar), the angle was measured upon dorsal or ventral placement of the paw on the ground after a swing phase or after a forward sweep of the paw over the beam surface. At each time point after SCI, 3–6 measurements were made for each hindlimb, that is, 6–12 "step cycles" that were defined according to the stepping ability of the animal as described above. The values for the left and right paw of each animal were averaged.

Selected frames were also used to measure RHI, a numerical estimate of the ability to support body weight, also an attribute of the BBB rating scale. RHI defined as the vertical distance from the dorsal aspect of the base of the animal's tail to the beam, normalized to the beam thickness measured along the same vertical line. For each animal and trial, the maximum RHI was estimated using video frames of 3–6 "step cycles," again defined according to stepping ability.

In addition, we analyzed video recordings of animals while climbing up an inclined ladder to count correct ladder steps (CLS), defined as correct placing of the hind paw and a briefly sustained position until the next forward step (24,27). In brief, after initial training, rats learned to climb up to the top of the ladder and even severely disabled animals after SCI could do so using their forelimbs and the body weight support provided by the inclined position of the ladder. The ladder-climbing test thus allows quantitative evaluation of complex motor behavior spanning normal function (noninjured) to complete paralysis. Video recordings were observed at slow-speed playback and the CLS placing of the hind paw and sustained position until the next forward move, counted. The pre-injury values varied between 7 and 9 rungs.

Bladder Function

Bladder function was assessed immediately prior to each manual voiding, that is, 2 times daily (~7:00 and 19:00 o'clock), using the following scoring method which has been described previously (24,25,36): Completely empty (no urine could be expressed, 0 points); half empty bladder containing several drops of clear urine (10 points); wet perineum, filled bladder with clear urine (20 points); half empty bladder with turbid urine (30 points); wet perineum, full bladder with turbid urine (40 points); half empty bladder with bloody urine (50 points); and wet perineum, full bladder with bloody urine (60 points). We analyzed data collected midweek for each week up to 12 weeks following SCI.

Thermal Sensitivity

Withdrawal latencies following thermal stimulation were measured before SCI (0 weeks) as well as at 1, 3, 6, 9, and 12 weeks thereafter. Animals were placed in a clear plastic chamber on a plastic table with a moveable laser device below it. The laser beam (2-mm diameter; temperature of 55°C) was directed over the plantar surface of the left and right hind paws and the ventral surface of the tail base. Once the laser was activated, sensors measured time in seconds as well as any movement of the hind limbs or tail away from the laser (Ugo Basile Thermal Plantar Analgesia Instrument, Stoelting Europe) thereby enabling measurement of withdrawal latency, that is, how long the beam was directed at the rat's hind limbs or tail before the animal reacted and moved away. Left and right hind paws, as well as the tail, were stimulated 3 times, and values were averaged (37–40). Our own previous results showed that there were no significant differences in the withdrawal latencies recorded from these 3 regions (25). This is why we initially stimulated the animals in all 3 regions 3 times and averaged the values. For a more detailed analysis, we considered all measurements separately.

Anatomical Assessments

Lesion Site

Spinal cord lesion length. Twelve weeks after SCI, rats were deeply anesthetized with Isoflurane (Forene, Abbott Laboratories) and perfused transcardially with phosphate buffered saline (PBS) for 30 seconds followed by 4% formaldehyde (Carl Roth, Karlsruhe, Germany) in 0.1 M PBS, pH 7.4, for 20 minutes. The spinal cord was dissected free between T7 and T9, cryoprotected (20% sucrose in PBS), cut in longitudinal cryo-sections (25 µm) in the frontal plane and mounted on SuperFrost Plus slides (Carl Roth). Each fifth longitudinal section was collected, yielding a total of at least 10 equidistant sections through the spinal cord of every animal, stained with cresyl violet (Carl Roth) and a fractionator sampling strategy used (41). Lesion lengths (in µm) from images of each section were measured at a primary magnification of ×2.5 using a microscope (Carl Zeiss, Oberkochen, Germany) equipped with a CCD Video Camera System (Optronics Engineering, Model DEI-470, Goleta, CA, supplied by Visitron Systems, Puchheim, Germany) combined with Image-Pro Plus 6.2 software (Media Cybernetics, Silver Spring, MD) (24,27). Measurements were performed by 2 observers blinded to the treatment groups.

Lesion Volume

Using the same images from longitudinal sections (i.e. at least 10 per animal), and the same hardware and software, we delineated and measured the lesion areas in μm^2 as described earlier (24,27). The total lesion volume was calculated by multiplying the measured area (in μm^2 by 25 µm [the thickness of the sections]), using the Cavalieri method (41).

Perilesional Tissue Bridge Area

Chronic contusion cavities are surrounded by perilesional tissue bridges (42). Using the same images, hardware and software as described above, we delineated and measured the areas of the PNTB in μm^2.

Antineuronal Class III β-Tubulin Immunoreactivity in Perilesional Tissue Bridges Immunohistochemistry

A separate set of 10 equidistant longitudinal cryosections through the lesion site of each animal were immunostained with 1:1000 polyclonal antineuronal class III β-tubulin (Covance, Richmond, CA, No. PRB-435P) and 1:400 anti-rabbit IgG Cy3 conjugate (1:400; Sigma-Aldrich, Merck, Darmstadt, Germany, No. C-2306). All sections were mounted on slides and incubated in identical solutions.

Sections were initially dried overnight at 37°C and rinsed the following day in PBS (0.1 M, pH 7.4) for 5 minutes at room temperature (RT). We used a method that allowed repeated use of antibody solutions which had been stabilized by the nongelling vegetable gelatin lambda-carrageenan (Sigma-Aldrich, Merck) and sodium azide (Sigma-Aldrich, Merck) (43). The method allows incubation of all sections from all rats in one jar, thereby ensuring high reproducibility.

The staining protocol has been described previously (44). Water-bath antigen demasking (antigen retrieval) was performed in 0.01 M sodium citrate (Sigma-Aldrich, Merck) solution, pH 9.0, for 30 minutes at 80°C (45). Nonspecific binding was blocked using 5% (v/v) normal serum from the species in which the secondary antibody was produced, dissolved in PBS, and supplemented with 0.2% (v/v) Triton X-100 (Sigma-Aldrich, Merck, CAS Number 9002-93-1; facilitates antibody penetration) and 0.02% (w/v) sodium azide (prevents microbial contamination) for 1 hour at RT. Incubation with the primary antibody (rabbit antineuronal class III β-tubulin [Covance, No. PRB-435P, 1:1000]) diluted in PBS containing 0.5% (w/v) λ-carrageenan (Sigma, CAS Number 9064-57-7; a nongelling vegetable gelatin, which reduces nonspecific binding and stabilizes the antibody solution) and 0.02% (w/v) sodium azide (Sigma, CAS Number 26628-22-8), was performed for 3 days at 4°C. After washing in PBS (3 times for 15 minutes at RT), the appropriate secondary antibody (anti-rabbit IgG Cy3 conjugate, Sigma, Sigma-Aldrich, Merck, No. C-2306) diluted 1:400 in PBS-carrageenan solution was applied for 2 hours at RT. After a subsequent wash in PBS, cell nuclei were stained for 10 minutes at RT with NeuroTrace 500/525 (1:200; Molecular Probes, N21480, via Life Technologies, Darmstadt, Germany). Finally, the sections were washed again, mounted in antifading medium (Fluoromount G; Southern Biotechnology Associates via Biozol, Germany), and stored in the dark at 4°C.

Microscopy. Sections were observed using a Zeiss Axioskop 50 epifluorescence microscope equipped with a "rhodamine" filter (excitation BP 546/12, beamsplitter FT 580, emission LP 590) and a stabilized powerful UV source (XBO 75W/HBO100W). Digital images were captured with a slow scan CCD camera (Spot RT, Diagnostic Instruments) using a ×2.5 objective.

The lesion site in rat comprises central cavitation, glial scar tissue and disrupted, demyelinated, and intact axons around the ventral and lateral periphery (46), In addition, tissue bridges containing axons extend from the spared rim into the cavity (42,47,48). Quantification was therefore performed using an image that encompassed the entire lesion and not selected areas of interest therein. All images were taken using an identical exposure duration.

Quantification of immunofluorescence after β-tubulin staining. Image files were opened with the Image-Pro Plus Software (Version 6.2; Media Cybernetics, Inc.). The borders of the PNTB were outlined using the "create polygon feature" of the "Measure" menu. Thereafter the number of red immunofluorescent profiles (representing structures that were positive for antineuronal class III β-tubulin) was quantified in each delineated image using the option "Count and Measure Objects" in the main menu. The intensity range selection (gray scale range) was adjusted to 128–255. "Automatic bright objects" as an objective and constant count mode was selected in the "Count/Size" option.

Statistical Analysis

The experiments generated diverse types of data that required different statistical analysis. Data were analyzed for differences in distribution and variance using ANOVA. Time-related changes were established using repeated measures ANOVA. For data that were measured once, and for comparisons between groups at specific time points, a one-way ANOVA was used followed by appropriate post hoc tests. Kruskal-Wallis one-way ANOVA on ranks followed by Dunn's post hoc test were performed if the sample variables violated the assumptions for the parametric ANOVA (neurotubulin-immunofluorescence) or the variable was measured on an ordinal scale (bladder status).

Statistical analyses of locomotor performance (BBB, FSA, RHI), spinal cord lesion volume and neurotubulin-immunofluorescence measurements were performed using Sigma Plot software (v.11 and 18; SPSS, Chicago, IL).

The effects of time after injury and the velocity of compression on functional outcomes, as well as the association between morphological and functional findings, were analyzed in the R language and environment for statistical computing (49).

In repeated measures factorial designs, such as used here, multiple comparisons at different time points may inflate the type I errors considerably. Thus, the effect of injury-type and time since injury on the multivariate functional outcome was confirmed by nonparametric multivariate ANOVA (50), followed by analysis of the univariate linear mixed effects models (51,52). The relationship between functional measurements and injury were fitted to a linear model of the general form:

$$Outcome \sim Value_{intact} + Trauma * (t + t^2) + (1|ID)$$

where *outcome* is the functional measurement in an animal with identity "*ID*" from a group "*Trauma*" in week "*t*" after the injury. $Value_{intact}$ is the value of the measurement in the intact state, that is, before the injury. The model includes a random intercept dependent on animal identity—"$1|ID$" in the logical formula. Intact values were omitted for the BBB and bladder scores since they are the same for all intact animals. Additionally, when assessing the bladder score (being an ordinal variable), the quantitative changes over time make little

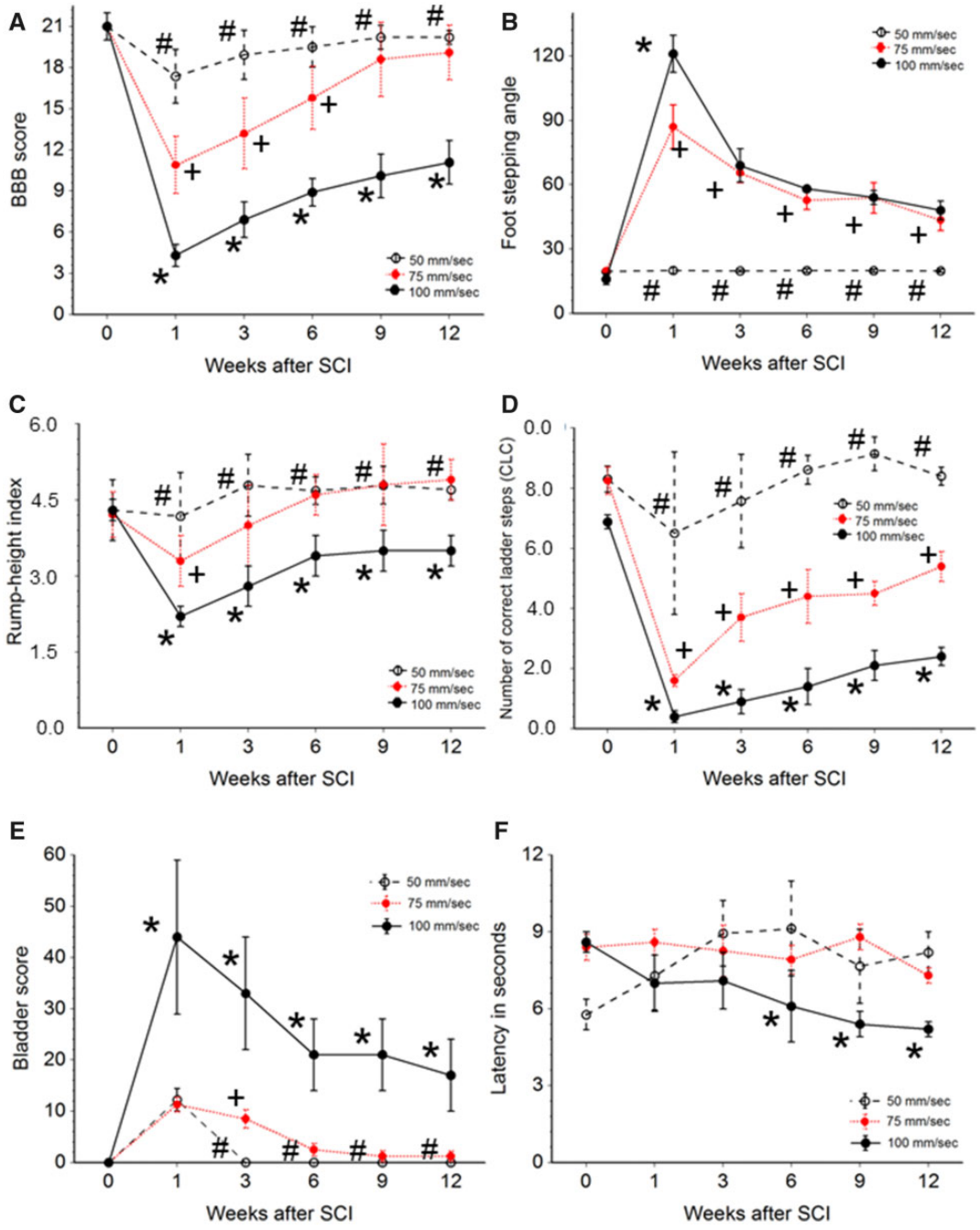

FIGURE 1. (A–F) Time course of values for several functional parameters. **(A)** Basso, Beattie, Bresnahan (BBB) motor scores; **(B)** foot stepping angle (FSA) in degrees; **(C)** rump-height index; **(D)** number of correct ladder steps; **(E)** bladder score (BS); **(F)** withdrawal time in seconds. Time 0 refers to pre-injury, that is, intact normal, values. Values are means ± standard deviation. Other abbreviations are as in Supplementary Data Table S1. Comparative analyses of the functional assessment were performed using Sigma Plot software. Differences with the selected level of statistical significance ($p \leq 0.05$) between group 100 mm/second ($n = 12$ rats) and group 75 mm/second ($n = 12$ rats) are indicated by *, between group 100 mm/second and group 50 mm/second ($n = 8$ rats) by $^{\#}$ and between groups 75 mm/second and group 50 mm/second by $^{+}$.

sense and therefore data for bladder score were fitted to a nonparametric mixed linear model using the nparLD library for R (53). The nonparametric model fits the rank of the bladder score as a response of the different severity of the injury and time after the intervention; an interaction term is also included. The BBB score is also an ordinal variable but it was shown that it behaves like normal continuous variable and can be analyzed with parametric tests (54).

The association between functional and morphological measurements was assessed by the correlation between each

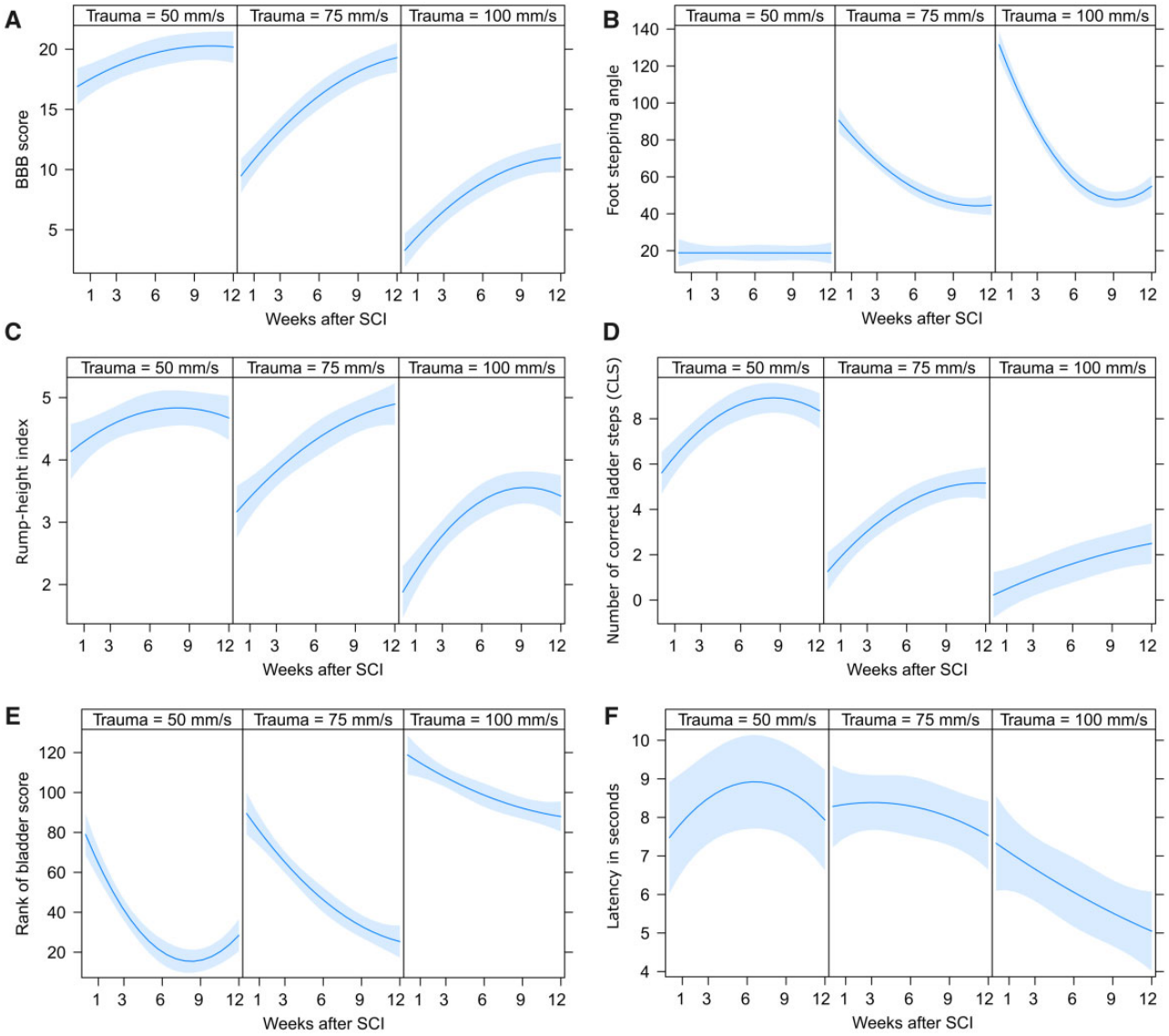

FIGURE 2. (A–F) Effects of the velocity of SCI (50 mm/second, 75 mm/second, or 100 mm/second) on the changes in the measured functional outcomes estimated by the mixed effects models. The shaded area indicates the 95% confidence interval of the estimates (blue line). The higher velocity of the injury leads to significantly worse intermediate and final results of the quantitative functional measurements Basso, Beattie, Bresnahan (BBB) score **(A)**, foot stepping angle **(B)**, rump-height index **(C)**, and number of correct ladder steps **(**CLS; **D)**. For BBB score **(A)** and CLS **(B)** this worsening is accompanied by decreased rate of recovery over time in the animals subjected to higher velocity injury. **(E)** The rank of the bladder score was fitted to a nonparametric model, which includes the same covariates as the other models. The graph shows the estimated change in rank of the ordinal bladder score over time. This outcome is not quantitative and should be interpreted only qualitatively, that is, the bladder score is expected to decrease (improve) over time but the animals that were subjected to higher velocity injuries are more likely to have higher bladder scores and probably slower improvement over time. **(F)** The estimated effects on the thermal sensitivity measured by the latency of withdrawal are more obscure. The most severe injury at 100 mm/second leads to substantial reduction in latency of withdrawal (increased sensitivity) after the SCI and a continuous decrease over time. Perhaps these values represent hypersensitivity and/or pain. The wider confidence intervals indicate that large portion of the variance was not explained by the model, that is, there could be other unknown factors influencing postinjury sensitivity.

functional and each morphological outcome. First, to ensure one-to-one mapping between functional and morphological outcomes, we calculated the "total functional outcome" for each functional measurement. The "total functional outcome" was presented by the estimates of the area under the curve for the observed period of 12 weeks. These estimates of "total function" were correlated with the morphological variables (55–57).

All data are presented as group mean ± standard deviation (SD) unless stated otherwise. For all statistical tests, the

significance level for acceptance of differences was set at $p \leq 0.05$.

RESULTS

Injury Model

Overall, and as detailed below, we found that only compression at 75 mm/second was suitable for our correlation analyses, whereas compression at 50 mm/second caused no long-term paraparesis and compression at 100 mm/second was not followed by functional recovery.

Functional Measurements

An initial nonparametric MANOVA examined the velocity of the trauma and the time after injury as independent variables and all functional measurements as dependent outcome (50). It showed a significant multivariate effect for the functional outcomes as a group in relation to both trauma velocity (Dempster's ANOVA = 55.21; $p < 0.001$) and time after injury (Dempster's ANOVA = 29.70; $p < 0.001$). Furthermore, the MANOVA detected a significant interaction of the 2 factors (Dempster's ANOVA = 9.07; $p < 0.001$) which can be interpreted as a sign that severity of the trauma changed the recovery rate over time as well. The univariate relationships between each functional outcome and the studied factors were fitted to linear mixed effects models. The full summaries for the models can be found in the Supplementary File.

Basso, Beattie, Bresnahan

As expected, in normal animals (i.e. preinjury), BBB scores were 21. As early as 1 week following injury, the scores (SCI-50: 17.4 ± 2.0; SCI-75: 10.9 ± 2.1; and SCI-100: 4.3 ± 0.8) showed that the different velocities of spinal cord compression produced injuries that caused different disabilities (7). Differences between the 3 groups could still be detected at 6 weeks after SCI. At the last 2 time points (9 and 12 weeks), the SCI-75 group improved so much that it almost reached the initial pre-injury values (19.1 ± 2.0). Accordingly, the mean BBB scores at 9 and 12 weeks differed only between the SCI-50 and SCI-100 groups (Supplementary Data Table S1; Fig. 1A). Over the 12 weeks of our observations, we detected statistically significant differences in the BBB between the 3 groups. In the SCI-50 group, we saw a slight drop to ~18 at 1 week, indicating a mild initial injury, followed by almost complete recovery by 3 weeks. By contrast, the SCI-100 was severe and did not show any recovery. In the SCI-75 group, we saw a reduction in the BBB score to 11 at week 1, followed by almost complete recovery (Supplementary Data Table S1; Fig. 1A). The data from the analysis of the statistical mixed model (Table 2) suggest that there is significant effect of the velocity of injury on both—the functional outcome and on the time related changes in BBB scores (the time dependent rate of change; Fig. 2A).

Foot Stepping Angle

FSAs of >90° indicate that the dorsal, rather than the plantar, surface of the toes or paw touch the ground during ground locomotion. Compared with pre-injury values (~18°), at 1 week following surgery, FSA was significantly higher in 2 groups (SCI-75: 87.0 ± 10.2°; SCI-100: 121.0 ± 8.6°; $p < 0.001$). At 3–12 weeks, values remained significantly higher than pre-injury at all time points ($p < 0.001$). The regression analysis showed that in both groups FSA improved partially over time (Table 2; Fig. 1B). In the first weeks after the injury, the FSA seemed to improve much faster in SCI-100 as compared with SCI-75. In the second half of the observation period, however, FSA in both groups did not improve substantially and no significant differences between the 2 groups could be detected ($p > 0.05$; Supplementary Data Table S1; Figs. 1B and 2B).

Rump-Height Index

RHI indicates the ability of the hindlimbs to support body weight during overground locomotion. Compared with pre-injury values (>4) at 1 week following surgery, RHI was significantly different in all 3 groups (SCI-50: 4.2 ± 0.9; SCI-75: 3.3 ± 0.5; and SCI-100: 2.2 ± 0.2; $p < 0.05$). In the following weeks, only the SCI-75 group showed improvement: The values for SCI-100 remained low (~3) and those for SCI-50 did not differ from the pre-injury ones (Supplementary Data Table S1; Fig. 1C). Regarding the RHI, the effects are

TABLE 1. Time Course of Withdrawal Latencies Measured in Both Hind Paws and in the Tail Base

Parameter/Animal Group	0 Weeks Preinjury	1 Week After SCI	3 Weeks After SCI	6 Weeks After SCI	9 Weeks After SCI	12 Weeks After SCI
Left hind paw: SCI-50	5,8 ± 0.8	7.2 ± 1.4	8.9 ± 1.4	9.4 ± 1.6	7.5 ± 1.5	8.1 ± 0.7
Left hind paw: SCI-75	8.3 ± 0.3	8.7 ± 0.4	8.9 ± 1.2	8.2 ± 0.5	8.7 ± 0.6	7.3 ± 0.9
Left hind paw: SCI-100	8.4 ± 0.2	6.9 ± 1.3	7.2 ± 1.4	6.2 ± 1.5	5.4 ± 0.5	5.2 ± 0.3
Right hind paw: SCI-50	5.7 ± 0.2	7.9 ± 1.2	9.1 ± 1.5	9.1 ± 2.1	7.7 ± 0.8	8.0 ± 0.9
Right hind paw: SCI-75	8.5 ± 0.7	8.4 ± 0.4	8.9 ± 0.7	8.3 ± 0.7	8.7 ± 0.4	7.7 ± 0.8
Right hind paw: SCI-100	9.0 ± 0.8	7.2 ± 1.4	7.3 ± 1.4	6.3 ± 1.5	5.4 ± 0.6	5.2 ± 0.3
Tail base: SCI-50	5.9 ± 0.6	6.8 ± 1.2	8.8 ± 1.1	8.9 ± 1.6	8.0 ± 1.9	8.6 ± 0.9
Tail base: SCI-75	8.4 ± 0.7	8.6 ± 0.0	7.3 ± 1.1	7.3 ± 0.5	8.8 ± 0.6	7.0 ± 1.4
Tail base: SCI-100	8.3 ± 0.4	7.1 ± 0.6	7.1 ± 0,6	5.9 ± 1.4	5.4 ± 0.6	5.2 ± 0.4

SCI, spinal cord injury.

more moderate. It is evident from the mixed effects model that not all variance in the RHI data can be explained by the effects of the injury type and the time since injury (Table 2; Fig. 2C). Here, we observed only main effects, that is, the more severe trauma lead to reduced RHI in the corresponding animals, but no substantial effect on the pattern of restoration over time could be detected (Table 2; Fig. 2C). One possible explanation of this phenomenon is that RHI might be influenced by 2 opposite processes. On the one hand, gradual restoration of motor control and recruitment of motor units might lead to improved weight support in the hind limbs and thus increase the RHI. On the other hand, it is feasible that spasm in the musculature of the hind legs caused by the loss of the corticospinal projections may affect the position of the caudal trunk and thus influence the measurement of the RHI.

Correct Ladder Steps

During inclined ladder climbing, both correct paw placement and maintaining them on the rungs to support body weight require high levels of motor and sensory control. Compared with pre-injury values (~7.0–8.5), at 1 week following surgery, the number of CLS was significantly reduced in all 3 groups (SCI-50: 6.5 ± 2.7; SCI-75: 1.6 ± 0.2; and SCI-100: 0.4 ± 0.2; $p < 0.001$). Thereafter, and similar to BBB and RHI (see above), only the SCI-75 group showed improvement, although not complete: Values for the SCI-50 group did not differ from those before SCI and values for the SCI-100 group only reached ~2 (Supplementary Data Table S1; Fig. 1D). Similarly to the BBB score, increasing the velocity of impact during SCI lead to worse functional outcomes and reduced the rate of functional restoration, especially in the group, injured at 100 mm/second (Table 2; Fig. 2D).

Bladder Function

Higher scores indicate worse function. Compared with pre-injury values (0), at 1 week, scores were significantly impaired (SCI-50: 12.2 ± 2.2; SCI-75: 11.3 ± 1.4; and SCI-100: 44 ± 15; $p < 0.001$) including some animals in all 3 groups who were unable to void spontaneously. Thereafter, the SCI-50 group showed a rapid and almost complete recovery by 3 weeks, the SCI-75 group showed a progressive recovery to almost normal by 6 weeks and, although the SCI-100 group improved somewhat, bladder function was compromised (Supplementary Data Table S1; Fig. 1E). These observations are supported by the results of the non-parametric statistical model (Table 2; Fig. 2E).

Thermal Sensitivity

Pre-injury thermal withdrawal latencies were similar for the left and right hind paws as well as for the tail base (range: 5.8 ± 0.6–8.6 ± 0.4 second) (Table 1). Compared with pre-injury latencies, values in the groups SCI-50 and SCI-75 did not change in any of the groups until the twelfth week after SCI. A significant reduction was detected in the SCI-100 group at weeks 6, 9, and 12 (Supplementary Data Table S1; Fig. 1F). At a first glance, it seems that there was no effect of injury severity or of time since injury (Fig. 1F). However, the mixed-

TABLE 2. Results From the Analysis of Mixed Effects and Nonparametric Models: ANOVA Type III Statistics for the Main Effects and Interactions of Evaluated Models of Functional Variability Over Time

	Main Effects		Interactions			Explanatory Power
Dependent Variable	Trauma	t	t^2	t*Trauma	t^2*Trauma	Marginal R^2
BBB	F (2; 65.2) = 85.8 p<0.001	F (1; 86) = 81.0 p<0.001	F (1; 86) = 22.4 p<0.001	F (2; 86) = 3.3 p=0.4	F (2; 86) = 0.36 p=0.69	0.89
FSA	F (2; 105) = 229.84 p<0.001	F (1; 105) = 128.5 p<0.001	F (1; 105) = 60.2 p<0.001	F (2; 105) = 44.0 p<0.001	F (2; 105) = 23.2 p<0.001	0.93
CLS	F (2; 68.3) = 36.0 p<0.001	F (1; 86) = 49.8 p<0.001	F (1; 86) = 20.0 p<0.001	F (2; 86) = 3.7 p=0.03	F (2; 86) = 3.4 p=0.04	0.90
RHI	F (2; 99.5) = 27.5 p<0.001	F (1; 86) = 35.5 p<0.001	F (1; 86) = 15.3 p<0.001	F (2; 86) = 1.57 p=0.21	F (2; 86) = 1.1 p=0.33	0.73
Bladder	F (1; 41, Inf) = 302 p<0.001	F (3; 15, Inf) = 90.6 p<0.001	–	F (4; 5, Inf) = 8.6 p<0.001	–	
Paw	F (2; 48.9) = 0.9 p=0.76	F (1; 78) = 0.7 p=0.40	F (1; 78) = 2.9 p=0.09	F (2; 78) = 3.16 p=0.04	F (2; 78) = 1.7 p=0.18	0.48

The bladder data were fitted to a nonparametric model.
BBB, Basso, Beattie, Bresnahan rating scale; FSA, foot-stepping angle; CLS, Correct Ladder Steps; RHI, rump-height index.

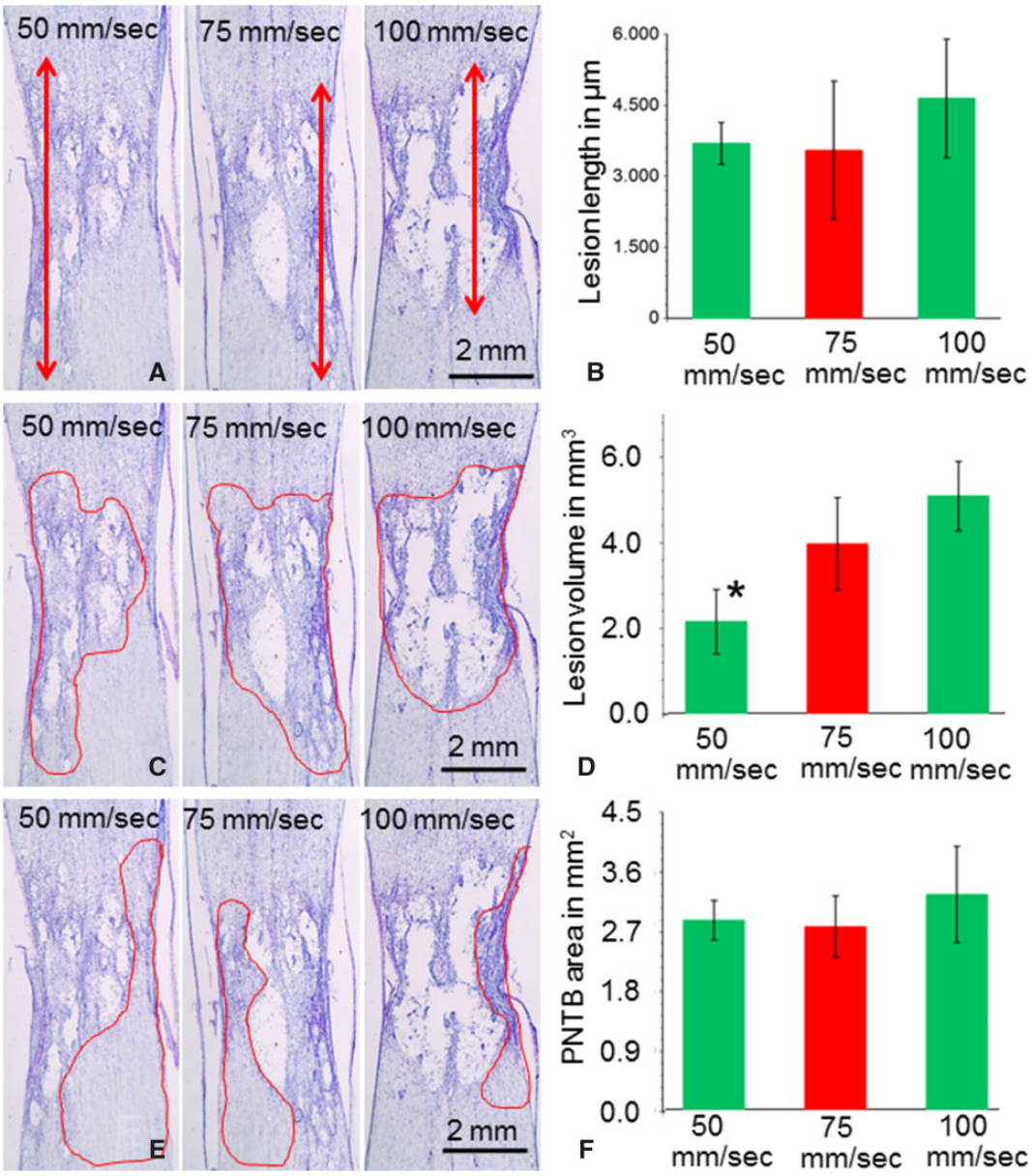

FIGURE 3. (A–E) Anatomical measurements in frontal longitudinal sections (25-µm thick) through the spinal cord from the 3 groups. The lesion site with the cavitation can be clearly identified. Ten serially spaced sections, which "covered" the entire thickness on the spinal cord, were stained with cresyl violet (Nissl stain) and used to measure the mean lesion length **(A)**, lesion volume **(**outlined cavity in **C)**, and area of the preserved neural tissue bridges **(**outlined bridges in **E)**. Quantitative estimates of the anatomical measurements. Values for each outcome are means ± standard deviation. There were no significant differences in the mean lesion length **(B)**, lesion volume **(D)**, and area of the preserved neural tissue bridges **(E)**, as assessed from cresyl-stained sections.

effects model takes into account the individual differences in thermal-withdrawal latency before injury. This allows us to observe an apparent progressive decrease in latency (progressive increase in pain sensitivity) in the 100 mm/second group as opposed to the groups with less severe SCI (Table 2; Fig. 4F). Thus, the most severe type of trauma is related to the worst sensitivity outcomes (pain) as well. The relatively high unexplained variance in the model (demonstrated by the wide confidence interval of the estimated effects; Fig. 2F) shows that there are clearly hidden factors influencing sensitivity/pain after SCI.

Taking all functional measurements into consideration, we conclude that injury in group SCI-50 was mild with complete recovery by week 3. By contrast, in the SCI-100 group, the injury was severe with no restoration of function. Nevertheless, in our subsequent anatomical analysis, we looked for

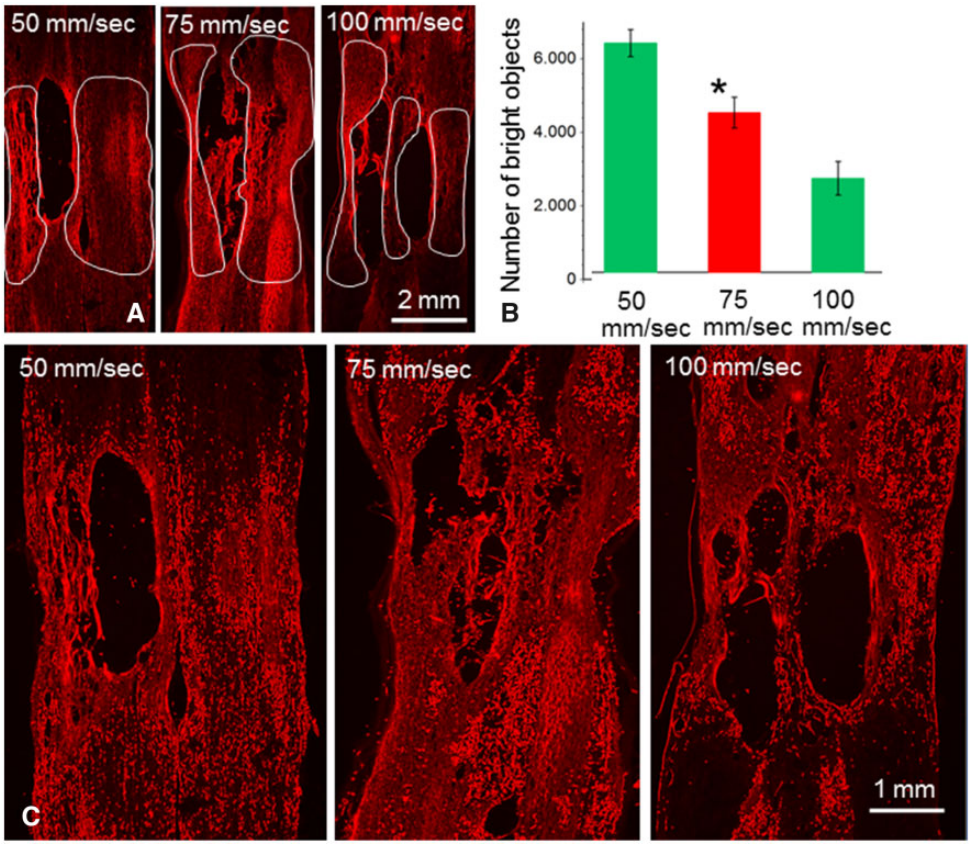

FIGURE 4. (A–C) Other sets of serially spaced sections were stained by immunofluorescence for neuronal class III β-tubulin and used to determine the amount of neural tissue in spared perilesional tissue bridges **(**outlined in **A)**. **(B)** Quantifications after immunofluorescent staining for neuronal class III β-tubulin showed that the amount of neural tissue in the spared perilesional tissue bridges (number of bright objects) in the SCI-75 group (n = 12 rats) was significantly higher when compared with that in the SCI-100 group (n = 12 rats). **(C)** The function "count number of bright objects" of the Image-Pro Plus Software, when applied to the images displayed in **A**, allowed documentation of images with relatively high-resolution profiles that were positive for antineuronal class III β-tubulin.

the morphological correlates of functional recovery in all groups, paying special attention to the comparison between the SCI-75 and SCI-100 groups.

Anatomical Measures

The multivariate ANOVA (F (4; 6) = 24.4; $p < 0.001$) suggests that at least one of the measured morphological outcomes is related to the severity of the SCI. There were no significant differences in the mean lesion length (between 3.5 and 4.5 mm; $p = 0.84$), and the area of preserved neural tissue bridges (PNTB; between 2.8 and 3.2 mm^2; $p = 0.67$) as assessed from cresyl-stained sections (Fig. 3A–F). In contrast, the volume of the lesion after the high-velocity SCI-100 (between 4.4 and 6 mm^3) was significantly higher than in the SCI-50 (1.4–3 mm^3; F (1; 9) = 10.9; $p = 0.009$). In trauma at moderate velocity (SCI-75), the resulting volume of the lesioned tissue (3.2–5 mm^3) was at intermediate levels between the other 2 groups and did not differ significantly from either.

The amount of neural tissue in spared perilesional tissue bridges assessed using staining of neuronal class III β-tubulin in the SCI-75 group (4485 ± 432) was significantly higher when compared with that in the SCI-100 group (2638 ± 471; F (1; 9) = 114.2; $p < 0.001$) (Fig. 4B).

We conclude that morphological parameters of SCI (lesion length, lesion volume and PNTB-area) are of limited prognostic value for the overall outcome. While there is a clear dependence of the lesion volume on the velocity of SCI, the differences are too subtle and cannot be used reliably for comparison between groups with small number of observations. Rather, the number of axons in neural tissue in spared perilesional tissue bridges may underpin restoration of function.

Correlation Between Functional Outcome and Morphological Changes

Finally, we checked for correlation between functional and morphological outcomes. To avoid the mapping functional measurements at different time points to singular morphological outcomes, we first described functional outcomes by a single value representative for the entire time course for

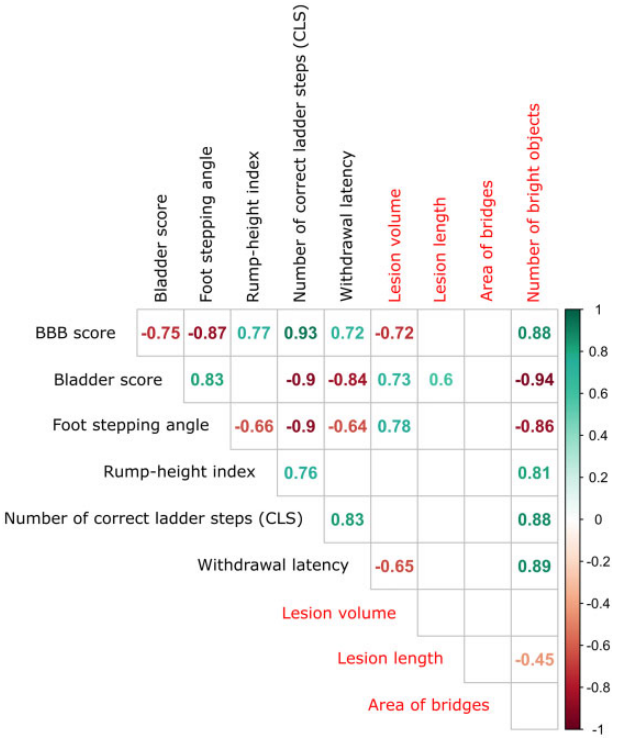

FIGURE 5. Multiple correlation matrix showing the Spearman's indices for correlation between the cumulative scores of the functional measurements (black; see explanations in text) and the measures for morphological changes (red) in the spinal cord after injury regardless of the velocity of the trauma. Only significant ($p \leq 0.05$) indices are shown. The color of the index denotes the direction of association: Green for positive correlation and red for negative. All functional measures are strongly correlated with each other, with the number of correct ladder steps (CLS) showing the highest correlation with all other functional outcomes. This is an indication that CLS could possibly be used as a single measurement for the evaluation of the complex locomotor function after SCI. Of the morphological measurements, only the number of bright objects shows strong correlation (absolute value above 0.8) with function. Lesion volume also correlates with some of the functional measurements but, interestingly, not with the rump-height index and CLS.

each animal. This value is the area enclosed under the curve limited by the first and last week of the corresponding measurement. An estimate for this area was calculated by the trapezoidal rule (58). The resultant score includes the variance from all single measurements (although the dynamics of the data are lost) and is a reasonable estimate for the "total function" during the period under investigation. FSA, RHI, CLS, and thermal withdrawal latency vary in intact animals. To account for this individual variation and to represent accurately the "total outcome" in FSA, RHI, CLS, and thermal withdrawal latency, we related the calculated area under the curve for these measures by the hypothetical total outcome expected in an Intact animal, which is equal to the length of the observed period of 12 weeks multiplied by the value measured in the intact animal.

For BBB and bladder score, we used the absolute values because (1) they are measured and expressed on an ordinal scale (which makes impossible the interpretation of relative measurements), and (2) the intact animals have the same values. The multiple correlations between the "total functional scores" and the morphological measurements are presented in Figure 5 and Table 3.

Only the lesion volume and the number of bright objects were found to significantly correlate with the functional measurements: (1) lesion volume with BBB and paw withdrawal latency (negatively), with FSA and bladder score (positively); and (2) number of bright objects correlated significantly with all cumulative functional measures with BBB, RHI, CLS, and withdrawal latency positively, while with FSA and bladder score negatively. Thus, it seems that it is the number of bright objects (representative for the number of axons), which is most significantly associated with the restoration of functional parameters.

DISCUSSION

The main results of our present study are 2-fold. First, by applying graded bilateral contusive injuries to the thoracic spinal cord (originally described by Curtis et al [28]), we found that only SCI at speed of 75 mm/second caused initial paraparesis with subsequent restoration of function. The contusion at a velocity of 100 mm/second caused a severe injury that was not followed by functional recovery whereas that at 50 mm/second was rather mild and caused only mild paraparesis. We therefore confirm earlier findings which show that survival of axons around the injury as well as motor, sensory, and vegetative recovery depend strongly on the impact velocity (59–62). The only case in which impact speed does not seem to determine severity of SCI has been reported after experiments with fixed impact displacement (63). Second, routinely used anatomical parameters, such as lesion volume, length and area of the perilesional tissue bridges did not correlate with degree of recovery at 12 weeks after SCI. Rather, the amount of neural tissue in the perilesional tissue bridges, as determined by antineuronal class III β-tubulin immunohistochemistry, correlated with functional recovery.

Are These Findings Really New?

We believe, yes. The last major study that correlated functional (BBB score), electro-physiological (motor evoked potentials and somatosensory evoked potentials), radiological (MRI: length of the cavity, lesion diameter, lesion area, cavity size, thickness of ventral and dorsal tissue bridges), and morphological (cross-sectional area of the spinal cord at the site of lesion, the amount of dorsal and ventral spared white matter) parameters after compressive SCI was published almost 20 years ago (64).

Moreover, our present results seem to be contradictory with those of Metz et al (64), who found a strong linear relation between MRI data (lesion length, spinal cord atrophy, spared white matter) to electrophysiological and functional

TABLE 3. Correlation Between Total Functional Outcomes and Morphological Measurements

		BBB	FSA	RHI	CLS	Paw	Bladder	Lesion Volume	Lesion Length	Area of Bridges	Number of Bright Objects
BBB	Spearman's rho	–	–0.867	0.769	0.93	0.725	–0.749	–0.721	–0.319	0.115	0.88
	p value	–	<0.001	<0.001	<0.001	0.003	<0.001	0.024	0.266	0.759	<0.001
FSA	Spearman's rho		–	–0.655	–0.896	–0.643	0.828	0.782	0.349	–0.382	–0.859
	p value		–	<0.001	<0.001	0.012	<0.001	0.012	0.221	0.279	<0.001
RHI	Spearman's rho			–	0.764	0.389	–0.402	0.067	–0.253	0.152	0.811
	p value			–	<0.001	0.152	0.123	0.865	0.382	0.682	<0.001
CLS	Spearman's rho				–	0.832	–0.902	–0.6	–0.169	0.261	0.881
	p value				–	<0.001	<0.001	0.073	0.563	0.47	<0.001
Paw	Spearman's rho					–	–0.838	–0.648	–0.088	–0.006	0.888
	p value					–	<0.001	0.049	0.746	1	<0.001
Bladder	Spearman's rho						–	0.729	0.603	–0.061	–0.938
	p value						–	0.011	0.008	0.859	<0.001
Lesion volume	Spearman's rho							–	0.045	0.073	–0.555
	p value							–	0.903	0.839	0.082
Lesion length	Spearman's rho								–	0.109	–0.45
	p value								–	0.755	0.019
Area of bridges	Spearman's rho									–	0.027
	p value									–	0.946
Number of bright objects	Spearman's rho										–
	p value										–

BBB, Basso, Beattie, Bresnahan rating scale; FSA, foot-stepping angle; CLS, Correct Ladder Steps; RHI, rump-height index.

(locomotor capacity) outcome parameters. Possible explanations to this discrepancy include the different lesion models between the 2 studies, with Metz et al using a weight-drop contusion, which is less precise than the compression model we used in this study (64). In addition, although these authors performed SCI with 3 different severities (6.25, 12.5, and 25 g/cm), specific functional and morphological consequences were not described for each group. Rather, they subdivided the injured rats into 3 groups based on severe (8–12), intermediate (13–16), or high (17–21) BBB score and did not relate these to injury severity. Moreover, the BBB scale was the only method that was used to determine locomotor activity. Although it includes a subset of readily observable attributes of gait and coordination, other attributes of locomotor recovery, such as speed of locomotion, paw area, stance width, and step cycle dynamics, are not addressed (65). In addition, limitations emerge from its categorical nature. Another possible explanation is that Metz et al used an interactive program for the MRI analysis that was written for the study rather than standardized software (64). Furthermore, rats were killed by decapitation, followed by dissection of the spinal cords, which may have led to lower quality histological material compared with tissue fixed by transcardial perfusion. In addition, immunohistochemical staining for neuronal markers tissue was not undertaken.

Aren't These Findings Obvious?

These findings could be considered as obvious if there is a direct relationship between the area of the perilesional tissue bridges and the amount of surviving, and presumably functional, neural tissue. However, the relationship is not straightforward. Previous studies have shown that the residual white matter that persists chronically after SCI (i.e. in the perilesional tissue bridges) is structurally abnormal, with a reduced density of, particularly larger diameter ($\geq$5 μm) axons, hypo and hypermyelination, as well as the presence of myelin debris and macrophages (47,66,67). Thus, the antineuronal class III β-tubulin-positive tissue comprises only a portion of that in the perilesional tissue bridges, presumably primarily preserved white matter. The remainder comprises, for example, reactive glia cells, oligodendrocytes and their precursors, immune cells and blood vessels (68), and it has recently been recognized that the biophysical properties of the damaged spinal cord also need to be considered (69).

Our findings are, in fact, in line with those of Basso et al, although indirectly (70). They also stated that "precise gradation in anatomical outcome was not apparent across all groups" (of varying lesion severities). Whereas Basso et al "confirmed that greater tissue sparing is highly correlated with final locomotor performance," they also emphasized that "very small increases in spared tissue at the lesion center had profound effects on basic locomotor recovery" and suggested "that sparing as few as 5%–10% of the fibers at the lesion center was sufficient to help drive the segmental circuits involved in the production of basic locomotion" (70). Since Basso et al did not study axon content, but the overall percentage of spared tissue, it cannot be concluded that the 5%–10% of spared tissue constituted only axons (70).

Another study also suggested that the anatomical evaluation of spared white matter is less effective for predicting functional outcome after SCI compared with lesion depth or the amount of spared white matter in the ventrolateral funiculus (34). Similar to Basso et al (70), they also concluded that a

small residual population of reticulospinal fibers can provide sufficient input to the lower spinal cord to initiate locomotor movements (34), but they did not study the axon content in this spared tissue.

What is the Clinical Relevance of These Findings, Especially in Regard to MRI?

Although the severity of damage after SCI is proportional to the amount of kinetic energy delivered by the mechanical impact, subsequent tissue alterations are not well understood (71). For example, human patients with large post-injury medullar cavities may recover well, regain micturition control and even start to walk, that is, the lesion area and the lesion volume are not significantly related to motor function (64). In addition, individual differences in pre-injury spinal cord morphometry influence functional and anatomical outcomes (72).

MRI, specifically T2-weighted, has become standard in the assessment of the injured spinal cord and is invaluable to achieving accurate diagnosis (73). Conventional MRI, however, has limited sensitivity to detect more subtle changes, for example in detecting inflammatory cerebrospinal fluid biomarkers that occur within the spinal cord after contusive injury in humans (74). Following dorsal column transection injury, however, quantitative MRI can accurately characterize white matter damage in the rat spinal cord (75).

Diffusion tensor imaging (DTI) has been applied to non-invasively detect structural changes and axonal damage in the central nervous system that occur in SCI (76,77). Whereas DTI has been shown to provide microstructural information on pathology in the spinal cord (78), clinical studies are informed by parameters that can be detected only noninvasively (79–83). Experimental studies, however, have begun to relate DTI to quantitative analysis of histological and immunohistochemical changes within the lesion following SCI (17,84–86). However, evidence suggests that inflammation, a hallmark of SCI (87), as well as axonal loss can confound the DTI assessment of axon or myelin injury (63,88). To eliminate these confounds, Lin et al developed diffusion basis spectrum imaging (DBSI) to separate the contributions of multiple coexisting pathologies that often exist in various white-matter diseases (89). Axonal loss detected by DBSI correlates well with clinical functional assessments, suggesting that DBSI could potentially serve as an outcome measure to predict neurological impairment after SCI.

ACKNOWLEDGMENTS

The skillful technical assistance of R. Jansen, Z. Isik, S. Wennmachers, S. Richter, K. Lütkemeier, and M.D. Gargari is highly appreciated.

REFERENCES

1. Wyndaele M, Wyndaele JJ. Incidence, prevalence and epidemiology of spinal cord injury: What learns a worldwide literature survey? Spinal Cord 2006;44:523–9
2. Hachem LD, Ahuja CS, Fehlings MG. Assessment and management of acute spinal cord injury: From point of injury to rehabilitation. J Spinal Cord Med 2017;40:665–75
3. Min YS, Park JW, Jin SU, et al. Alteration of resting-state brain sensorimotor connectivity following spinal cord injury: A resting-state functional magnetic resonance imaging study. J Neurotrauma 2015;32:1422–7
4. David G, Seif M, Huber E, et al. In vivo evidence of remote neural degeneration in the lumbar enlargement after cervical injury. Neurology 2019;92:e1367–77
5. Fouad K, Pearson K. Restoring walking after spinal cord injury. Prog Neurobiol 2004;73:107–26
6. Calvert JS, Grahn PJ, Zhao KD, et al. Emergence of epidural electrical stimulation to facilitate sensorimotor network functionality after spinal cord injury. Neuromodulation 2019;22:244–52
7. Basso DM, Beattie MS, Bresnahan JC. A sensitive and reliable locomotor rating scale for open field testing in rats. J Neurotrauma 1995;12:1–21
8. Gale K, Kerasidis H, Wrathall JR. Spinal cord contusion in the rat: Behavioral analysis of functional neurologic impairment. Exp Neurol 1985;88:123–34
9. Ko HY, Ditunno JF Jr, Graziani V, et al. The pattern of reflex recovery during spinal shock. Spinal Cord 1999;37:402–9.
10. Pikov V, Gillis RA, Jasmin L, et al. Assessment of lower urinary tract functional deficit in rats with contusive spinal cord injury. J Neurotrauma 1998;15:375–86
11. Bresnahan JC, King JS, Martin GF, et al. A neuroanatomical analysis of spinal cord injury in the rhesus monkey (*Macaca mulatta*). J Neurol Sci 1976;28:521–42
12. Bresnahan JC. An electron-microscopic analysis of axonal alterations following blunt contusion of the spinal cord of the rhesus monkey (*Macaca mulatta*). J Neurol Sci 1978;37:59–82
13. Bresnahan JC, Beattie MS, Todd FD 3rd, et al. A behavioral and anatomical analysis of spinal cord injury produced by a feedback-controlled impaction device. Exp Neurol 1987;95:548–70.
14. Guizar-Sahagun G, Grijalva I, Madrazo I, et al. Development of post-traumatic cysts in the spinal cord of rats-subjected to severe spinal cord contusion. Surg Neurol 1994;41:241–9
15. Noble LJ, Wrathall JR. Spinal cord contusion in the rat: Morphometric analyses of alterations in the spinal cord. Exp Neurol 1985;88:135–49
16. Noble LJ, Wrathall JR. Correlative analyses of lesion development and functional status after graded spinal cord contusive injuries in the rat. Exp Neurol 1989;103:34–40
17. Zhao C, Rao JS, Pei XJ, et al. Diffusion tensor imaging of spinal cord parenchyma lesion in rat with chronic spinal cord injury. Magn Reson Imaging 2018;47:25–32
18. Becerra JL, Puckett WR, Hiester ED, et al. MR-pathologic comparisons of wallerian degeneration in spinal cord injury. AJNR 1995;16:125–33
19. Bunge RP, Clinical implications of recent advances in neurotrauma research. In: Salzman, SA, Faden, AI, eds. The Neurobiology of CNS Trauma. New York: Oxford University Press 1994:329–39
20. Bunge RP, Puckett WR, Becerra JL, et al. Observations of the pathology of human spinal cord injury. A review and classification of 22 new cases with details from a case of chronic cord compression with extensive focal demyelination. Adv Neurol 1993;59:75–89
21. Kakulas BA. Pathology of spinal injuries. Cent Nerv Syst Trauma 1984;1:117–29
22. Alizadeh A, Dyck SM, Karimi-Abdolrezaee S. Traumatic spinal cord injury: An overview of pathophysiology, models and acute injury mechanisms. Front Neurol 2019;10:282
23. Al Huthaifi F, Krzak J, Hanke T, et al. Predictors of functional outcomes in adults with traumatic spinal cord injury following inpatient rehabilitation: A systematic review. J Spinal Cord Med 2017;40:282–94
24. Wirth F, Schempf G, Stein G, et al. Whole-body vibration improves functional recovery in spinal cord injured rats. J. Neurotrauma 2013;30:453–68
25. Meyer C, Bendella H, Rink S, et al. The effect of myelotomy following low thoracic spinal cord compression injury in rats. Exp Neurol 2018;306:10–21
26. Rink S, Arnold D, Wöhler A, et al. Recovery after spinal cord injury by modulation of the proteoglycan receptor PTPσ. Exp Neurol 2018;309:148–59
27. Semler J, Wellmann K, Wirth F, et al. Objective measures of motor dysfunction after compression spinal cord injury in adult rats: Correlations with locomotor rating scores. J Neurotrauma 2011;28:1247–58
28. Curtis R, Green D, Lindsay RM, et al. Up-regulation of GAP-43 and growth of axons in rat spinal cord after compression injury. J Neurocytol 1993;22:51–64

29. Manthou M, Abdulla DS, Pavlov SP, et al. Whole body vibration (WBV) following spinal cord injury (SCI) in rats: Timing of intervention. RNN 2017;35:185–216
30. Waibl H. Zur Topographie der medulla spinalis der Albinoratte (*Rattus norvegicus*). Adv Anat Embryol Cell Biol 1973;47
31. Forgione N, Karadimas SK, Foltz WD, et al. Bilateral contusion-compression model of incomplete traumatic cervical spinal cord injury. J Neurotrauma 2014;31:1776–88
32. Hurd C, Weishaupt N, Fouad K. Anatomical correlates of recovery in single pellet reaching in spinal cord injured rats. Exp Neurol 2013;247: 605–14
33. Loy DN, Talbott JF, Onifer SM, et al. Both dorsal and ventral spinal cord pathways contribute to overground locomotion in the adult rat. Exp Neurol 2002;177:575–80
34. Schucht P, Raineteau O, Schwab ME, et al. Anatomical correlates of locomotor recovery following dorsal and ventral lesions of the rat spinal cord. Exp Neurol 2002;176:143–53
35. Steeves JD, Jordan LM. Localization of a descending pathway in the spinal cord which is necessary for controlled treadmill locomotion. Neurosci Lett 1980;20:283–8
36. Ramsey JB, Ramer LM, Inskip JA, et al. Care of rats with complete high-thoracic spinal cord injury. J Neurotrauma 2010;27:1709–22
37. Carlton SM, Du J, Tan HY, et al. Peripheral and central sensitization in remote spinal cord regions contribute to central neuropathic pain after spinal cord injury. Pain 2009;147:265–76
38. Chew DJ, Murrell K, Carlstedt T, et al. Segmental spinal root avulsion in the adult rat: A model to study avulsion injury pain. J Neurotrauma 2013; 30:160–72
39. Hargreaves K, Dubner R, Brown F, et al. A new and sensitive method for measuring thermal nociception in cutaneous hyperalgesia. Pain 1988;32: 77–88
40. Takahashi Y, Chiba T, Kurokawa M, et al. Dermatomes and the central organization of dermatomes and body surface regions in the spinal cord dorsal horn in rats. J Comp Neurol 2003;462:29–41
41. Gundersen HJ, Bendtsen TF, Korbo L, et al. Some new, simple and efficient stereological methods and their use in pathological research and diagnosis. APMIS 1988;96:379–94
42. Hill CE, Beattie MS, Bresnahan JC. Degeneration and sprouting of identified descending supraspinal axons after contusive spinal cord injury in the rat. Exp Neurol 2001;171:153–69
43. Sofroniew MV, Schrell U. Long-term storage and regular repeated use of diluted antisera in glass staining jars for increased sensitivity, reproducibility, and convenience of single- and two-color light microscopic immunocytochemistry. J Histochem Cytochem 1982;30:504–11
44. Irintchev A, Rollenhagen A, Troncoso E, et al. Structural and functional aberrations in the cerebral cortex of tenascin-C deficient mice. Cereb Cortex 2005;15:950–62
45. Jiao Y, Sun Z, Lee T, et al. A simple and sensitive antigen retrieval method for free-floating and slide-mounted tissue sections. J Neurosci Methods 1999;93:149–62
46. Chen K, Liu J, Assinck P, et al. Differential histopathological and behavioral outcomes eight weeks after rat spinal cord injury by contusion, dislocation, and distraction mechanisms. J Neurotrauma 2016;33:1667–84
47. Beattie MS, Bresnahan JC, Komon J, et al. Endogenous repair after spinal cord contusion injuries in the rat. Exp Neurol 1997;148:453–63
48. Quencer RM, Bunge RP. The injured spinal cord: Imaging, histopathologic clinical correlates, and basic science approaches to enhancing neural function after spinal cord injury. Spine (Phila Pa 1976) 1996;21:2064–6
49. R Core Team. R: A Language and Environment for Statistical Computing. Vienna, Austria: R Foundation for Statistical Computing. 2014. Available from: http://www.R-project.org. Accessed June 14, 2018
50. Kiefel M, Bathke AC. NparMD: Nonparametric analysis of multivariate data in factorial designs. 2018. Available from: https://CRAN.R-project.org/package=nparMD. Accessed June 14, 2018.
51. Bates D, Mächler M, Bolker B, et al. Fitting linear mixed-effects models using Lme4. J Stat Softw 2015;67:1–48
52. Kuznetsova A, Brockhoff PB, Christensen R. LmerTest package: Tests in linear mixed effects models. J Stat Softw 2017;82:1–26
53. Noguchi K, Gel YR, Brunner E, et al. NparLD: An R software package for the nonparametric analysis of longitudinal data in factorial experiments. J Stat Softw 2012;50:1–23
54. Scheff SW, Saucier DA, Cain ME. A statistical method for analyzing rating scale data: The BBB locomotor score. J Neurotrauma 2002;19:1251–60
55. Harrell FE Jr. *With Contributions from Charles Dupont and Many Others*. Hmisc: Harrell miscellaneous. 2019. Available from: https://CRAN.R-project.org/package=Hmisc. Accessed January 27, 2019
56. Selker R, Love J, Dropmann D. Jmv: The "jamovi" analyses. 2019. Available from: https://CRAN.R- project.org/package=jmv. Accessed April 22, 2019
57. Wei T, Simko V. R package 'corrplot': Visualization of a correlation matrix. 2017. Available from: https://github.com/taiyun/corrplot. Accessed October 17, 2017
58. Burden RL, Douglas Faires J. Numerical differentiation and integration. In: *Numerical Analysis*, ninth ed., Chapter 4. Pacific Grove, Australia: Cengage Learning, Brooks/Cole 2011:173–258
59. Sparrey CJ, Choo AM, Liu J, et al. The distribution of tissue damage in the spinal cord is influenced by the contusion velocity. Spine (Phila Pa 1976) 2008;33:E812–9
60. Kearney PA, Ridella SA, Viano DC, et al. Interaction of contact velocity and cord compression in determining the severity of spinal cord injury. J Neurotrauma 1988;5:187–208
61. Choo AM, Liu J, Liu Z, et al. Modeling spinal cord contusion, dislocation, and distraction: Characterization of vertebral clamps, injury severities, and node of Ranvier deformations. J Neurosci Methods 2009;181:6–17
62. Lam CJ, Assinck P, Liu J, et al. Impact depth and the interaction with impact speed affect the severity of contusion spinal cord injury in rats. J Neurotrauma 2014;31:1985–97
63. Kim JH, Tu TW, Bayly PV, et al. Impact speed does not determine severity of spinal cord injury in mice with fixed impact displacement. J Neurotrauma 2009;26:1395–404
64. Metz GA, Curt A, van de Meent H, et al. Validation of the weight-drop contusion model in rats: A comparative study of human spinal cord injury. J Neurotrauma 2000;17:1–17
65. Krizsan-Agbas D, Winter MK, Eggimann LS, et al. Gait analysis at multiple speeds reveals differential functional and structural outcomes in response to graded spinal cord injury. J Neurotrauma 2014;31:846–56
66. Bunge MB. Bridging areas of injury in the spinal cord. Neuroscientist 2001;7:325–39
67. Rosenberg LJ, Zai LJ, Wrathall JR. Chronic alterations in the cellular composition of spinal cord white matter following contusion injury. Glia 2005;49:107–20
68. Tran AP, Warren PM, Silver J. The biology of regeneration failure and success after spinal cord injury. Physiol Rev 2018;98:881–917
69. Moeendarbary E, Weber IP, Sheridan GK, et al. The soft mechanical signature of glial scars in the central nervous system. Nat Commun 2017;8: 14787
70. Basso DM, Beattie MS, Bresnahan JC. Graded histological and locomotor outcomes after spinal cord contusion using the NYU weight-drop device versus transection. Exp Neurol 1996;139:244–56
71. Mattucci S, Speidel J, Liu J, et al. Basic biomechanics of spinal cord injury—How injuries happen in people and how animal models have informed our understanding. Clin Biomech (Bristol Avon) 2019;64:58–68
72. Kim KT, Streijger F, So K, et al. Differences in morphometric measures of the uninjured porcine spinal cord and dural sac predict histological and behavioral outcomes after traumatic spinal cord injury. J Neurotrauma 2019;36:3005–17
73. Talbott JF, Huie JR, Ferguson AR, et al. MR imaging for assessing injury severity and prognosis in acute traumatic spinal cord injury. Radiol Clin North Am 2019;57:319–39
74. Dalkilic T, Fallah N, Noonan VK, et al. Predicting injury severity and neurological recovery after acute cervical spinal cord injury: A comparison of cerebrospinal fluid and magnetic resonance imaging biomarkers. J Neurotrauma 2018;35:435–45
75. Kozlowski P, Raj D, Liu J, et al. Characterizing white matter damage in rat spinal cord with quantitative MRI and histology. J Neurotrauma 2008;25:653–76
76. Beaulieu C. The basis of anisotropic water diffusion in the nervous system—A technical review. NMR Biomed 2002;15:435–55
77. Patel SP, Smith TD, VanRooyen JL, et al. Serial diffusion tensor imaging in vivo predicts long-term functional recovery and histopathology in rats following different severities of spinal cord injury. J Neurotrauma 2016; 33:917–28

78. Kim JH, Loy DN, Wang Q, et al. Diffusion tensor imaging at 3 hours after traumatic spinal cord injury predicts long-term locomotor recovery. J Neurotrauma 2010;27:587–98
79. Demir A, Ries M, Moonen CT, et al. Diffusion-weighted MR imaging with apparent diffusion coefficient and apparent diffusion tensor maps in cervical spondylotic myelopathy. Radiology 2003;229:37–43
80. Ellingson BM, Schmit BD, Kurpad SN. Lesion growth and degeneration patterns measured using diffusion tensor 9.4-T magnetic resonance imaging in rat spinal cord injury. SPI 2010;13:181–92
81. Facon D, Ozanne A, Fillard P, et al. MR diffusion tensor imaging and fiber tracking in spinal cord compression. AJNR 2005;26:1587–94
82. Lewis MJ, Cohen EB, Olby NJ. Magnetic resonance imaging features of dogs with incomplete recovery after acute, severe spinal cord injury. Spinal Cord 2018;56:133–41
83. Lewis MJ, Yap PT, McCullough S, et al. The relationship between lesion severity characterized by diffusion tensor imaging and motor function in chronic canine spinal cord injury. J Neurotrauma 2018;35:500–7
84. Sundberg LM, Herrera JJ, Narayana PA. In vivo longitudinal MRI and behavioral studies in experimental spinal cord injury. J Neurotrauma 2010;27:1753–67
85. Kaushal M, Shabani S, Budde M, et al. Diffusion tensor imaging in acute spinal cord injury: A review of animal and human studies. J Neurotrauma 2019;36:2279–86
86. Poplawski MM, Alizadeh M, Oleson CV, et al. Application of diffusion tensor imaging in forecasting neurological injury and recovery after human cervical spinal cord injury. J Neurotrauma 2019;36:3051–61
87. Hausmann ON. Post-traumatic inflammation following spinal cord injury. Spinal Cord 2003;41:369–78
88. Bjartmar C, Wujek JR, Trapp BD. Axonal loss in the pathology of MS: Consequences for understanding the progressive phase of the disease. J Neurol Sci 2003;206:165–71
89. Lin TH, Sun P, Hallman M, et al. Noninvasive quantification of axonal loss in the presence of tissue swelling in traumatic spinal cord injury mice. J Neurotrauma 2019;36:2308–15